Available online at www.CivileJournal.org

Civil Engineering Journal

(E-ISSN: 2476-3055; ISSN: 2676-6957)

Vol. 11, No. 08, August, 2025

Optimal Placement of Vibration Control Systems in a Smart Civil Engineering Structure

Houssameddine Chitaoui [1*], Abdellatif Megnounif [1], Zahira Benadla [1]

[1] *Risk Assessment and Management Laboratory, Faculty of Technology, University of Tlemcen, Chetouane B.P.230, 13000, Algeria.*

Received 13 April 2025; Revised 19 July 2025; Accepted 27 July 2025; Published 01 August 2025

Abstract

Advancements in construction technologies have led to the development of lighter and more flexible structures, which pose new challenges in terms of seismic resistance. This study explores the effectiveness of integrating an Active Tendon (AT) control system to mitigate seismic-induced vibrations in tall buildings. The main objective is to identify the optimal placement of these active control devices to maximize structural performance. To this end, three optimization approaches are investigated: modal controllability analysis, controllability index evaluation, and genetic algorithm (GA)-based optimization. The methodological approach is based on the development of a comprehensive flowchart that integrates the optimization procedures alongside a comparative assessment of passive and active control strategies. Detailed simulations were carried out in MATLAB, enabling accurate time-history analyses and the implementation of customized control algorithms. This framework enables extensive parametric studies and supports a rigorous assessment of control system performance. The results clearly show that optimal tendon placement leads to a substantial improvement in vibration mitigation compared to uncontrolled cases. Comparative analyses underscore the respective strengths and applicability domains of each optimization method, confirming their effectiveness in identifying optimal actuator locations. The novelty of this study lies in the integration of modal and evolutionary optimization techniques within a unified framework, offering a systematic and versatile approach to the placement of control systems in civil engineering structures. The practical recommendations derived from this study provide valuable guidance for engineers and designers seeking to improve structural performance under seismic loading.

Keywords: Structural Control; Optimization; Smart; Mitigation; Genetic Algorithm; Modal Controllability; Controllability Index.

1. Introduction

Earthquakes represent a major challenge for society and national development, often causing the collapse of civil engineering structures, significant human casualties, and substantial economic losses. Recent advances in design and construction materials have led to the emergence of lighter structural systems. While advantageous in many respects, these lighter structures are more susceptible to dynamic excitation, particularly in seismic or high-wind regions, which can lead to structural damage or discomfort for occupants. This underscores the necessity of integrating an adequate number of active, semi-active, or hybrid control systems in tall buildings to effectively reduce seismic responses. The performance of such systems is highly dependent on their strategic placement within the structure. Identifying the optimal locations for these devices—out of a large number of possible configurations—poses a complex optimization problem. This challenge can be addressed using either simple heuristic approaches or more advanced optimization techniques. Active and semi-active control systems have demonstrated high efficiency in vibration mitigation across a broad frequency spectrum, making them promising solutions for enhancing the seismic resilience of modern structures.

* Corresponding author: houssameddine.chitaoui@univ-tlemcen.dz

http://dx.doi.org/10.28991/CEJ-2025-011-08-022

Yanik et al. [1] are among the first to simultaneously incorporate active control, vibration control, and energy management in their research. The study analyzes the dynamic behavior and energy distribution in structures equipped with both passive and active control elements. The findings reveal that adding control devices significantly reduces structural dis-placements. However, implementing passive or active controls on an uncontrolled structure increases overall energy consumption. Berglund et al. [2] discussed the challenges in applying smart city technologies to manage aging infrastructure and meet growing urban demands. They reviews various smart technologies such as sensors, crowdsourcing, actuators, big data, and block chain, and their applications in civil engineering domains like transportation, water systems, and energy management. The paper identifies gaps in smart infrastructure implementation and proposes new roles for civil engineers in the development of smart cities, encompassing design, environmental and societal stewardship, innovation, risk management, and leadership in policymaking. An experimental study is used for numerical validation as a reference. Ramírez-Neria et al. [3] introduced an active vibration control technique for buildings during seismic events, utilizing active disturbance rejection control with a generalized proportional-integral observer to estimate and counteract unknown dynamics and disturbances. This approach, which doesn't require system parameters, offers robustness against disturbances and uncertainties. It also features an online robust adaptive observer to estimate immeasurable displacement and velocity, enhancing the control's effectiveness. Experimental results on a five-story scale model validate the method's potential for practical application.

Several recent approaches combine metaheuristic methods and artificial intelligence to optimize active control systems. Askari et al. [4] address the problem of optimal and economical placement of active actuators and magnetorheological (MR) dampers in nonlinear structures. They use a multi-objective genetic algorithm to determine the ideal number and placement of actuators in order to simultaneously minimize structural drift, acceleration, and base shear. Their results demonstrate that optimized positioning allows for a significant reduction in dynamic response compared to a standard arrangement. Jasiński et al. [5] address the issue of spatial optimization of tendons in statically indeterminate structures. They employ a hybrid method combining artificial neural networks to estimate initial configurations with a genetic algorithm for refining optimal positions. Their results indicate a notable improvement in accuracy and computation time thanks to this intelligent combination. Block et al.[6] focus on the 3D optimization of the arrangement of external tendons in prestressed structures, specifically taking into account losses due to friction, creep, and shrinkage. Using a method of optimization based on the minimization of deformation energy, their research leads to optimal configurations that effectively limit prestress losses, thereby significantly reducing residual moments. Jiwapatria et al. [7] addresses the challenge of optimal placement coupled with the tuning of parameters for active control systems subjected to severe dynamic excitations. They adopt an improved variant of the NSGA-II genetic algorithm guided by the population (PMR-NSGA-II). This approach allows for rapid convergence and effective reduction of dynamic responses compared to the classic NSGA-II, thus proving its superiority in complex multi-objective contexts. Zhao and Gu [8] study the optimization of LQR controller parameters in active automotive suspension systems to minimize undesirable vibrations. Their hybrid approach, combining a PSO (Particle Swarm Optimization) algorithm with a genetic algorithm (GA), provides a robust optimal solution. The results obtained show a significant reduction in acceleration, dynamic constraints, and loads on the suspension compared to a conventional LQR controller.

Numerous studies have been conducted on the optimal positioning of actuators for actively controlling seismic vibrations in tall structures using optimization algorithms. Li et al. [9] focused on optimizing the design of actuators shapes and locations in controlled structures, discussing the characteristics of the design problem and introducing a dual-stage genetic algorithm to address this challenge. Rama Mohan Rao & Sivasubramanian [10], the authors have introduced a Multi-Start Meta-heuristic algorithm (MSGNS), known as the multiple initiation guided neighborhood search algorithm, to investigate the best actuator position within active control designs. This research examines how four optimization criteria react to various earthquake records. While efforts have been made to determine the optimal placement of actuators and dampers based on optimization criteria, further research is necessary to fully comprehend this issue. Numerous other researchers have addressed the challenge of locating actuators and shock absorbers in structural vibration control systems. The common point in both Pourzeynali et al. [11] and Salvi et al. [12], a comparison of control strategies using Tuned Mass Dampers (TMD) and Active Tuned Mass Dampers (ATMD) was conducted, considering both controlled structures with and without SSI. The control force for the TMD was calculated using a Linear Quadrature Regulator (LQR) combined with a hybrid approach involving fuzzy logic and genetic algorithms. The proposed approach effectively reduces seismic displacements and velocities, better than a passive TMD or an LQR controller, although requiring higher control forces.

Gutierrez Soto & Adeli [13], their study focuses on recent literature regarding the optimal placement of passive, semi-active, active, and hybrid control devices for structural vibration control under dynamic loads, emphasizing the goal of enhancing performance cost-effectively and highlighting the need for further research into semi-active and hybrid controls for large, complex structures. Their recommendations emphasize that for a 6-story building, 36 devices on the top 4 floors reduce the response by 49%, and for a 24-story building, 72 devices on the top 10 floors achieve a 60% reduction. A multi-objective genetic algorithm with gene manipulation was introduced in Cha et al. [14] to optimize the placement of control devices and sensors in frame structures, aiming to reduce costs and enhance control strategies.

This methodology optimizes device distribution while minimizing structural drift in a 20-story building under seismic activity. It offers efficient device and sensor layouts, requiring up to 40% fewer generations without compromising solution quality. The effect of 18 different excitation forces on the optimal placement of actuators to reduce the largest displacement of the upper floor was studied in Liu et al. [15]. The results showed that the placement is not influenced by the level of earthquake. The authors propose an efficient method using a genetic algorithm for determining optimal actuator positions in tall buildings by formulating a discrete and nonlinear optimization problem. Cheng et al. [16], published an article on the optimal positioning of actuators and dampers was published, proposing a stochastic approach to solve the general optimization problem and developing a solution procedure. They demonstrated that a seismic response control system with optimally placed devices is significantly more effective than a system where device placement is not optimized, making it more practical.

Wani & Tantray [17], introduced adaptive control strategies for optimizing the placement and design of Magneto Rheological (MR) dampers in civil structures to reduce inter-story drift and acceleration responses. These strategies offer flexibility, allowing customization based on specific performance criteria and available control devices. Numerical simulations of a five-story frame structure demonstrate that optimal damper placement, informed by response-based control objectives, significantly enhances structural resilience during seismic events, outperforming standard genetic algorithm configurations with H_2/LQG controllers. Yanik et al. [18], tackle the shortcomings of traditional active control algorithms—typically designed for two-dimensional structural systems—by proposing an innovative performance index tailored for active vibration control in three-dimensional frameworks. This newly introduced index was analytically assessed through a case study involving a six-story 3D structure equipped with a fully active tendon control system, applying a tiered structural model to facilitate the dynamic analysis. The proposed index surpasses the classic optimal linear control and provides a better reduction in displacements, velocities, rotations, and energy responses. This new algorithm is more efficient because it requires no prior knowledge of the earthquake and is realistically applicable to 3D buildings. Zhang et al. [19], proposed a novel approach for actuator placement, addressing limitations in common methods by considering modal controllability degrees based on the Clough–Penzien spectral model and Luenberger observable normal form. Optimal actuator placement was determined through simulations on a 20-story building model, demonstrating superior vibration reduction compared to uniform distribution and classical placement methods based on the system controllability gramian matrix. The results demonstrate that the combined consideration of controllability and modal energy, as well as the MDM/SDM classification, leads to a more efficient placement of actuators, with substantial reductions in seismic response and improved system efficiency compared to traditional methods.

Rather & Alam [20], focused on modeling and control design for active vibration control of structures under seismic load, specifically for a 10-story frame structure with strategically placed tendons for optimal efficiency. Through numerical simulation in Simulink, the paper demonstrates significant response reduction and control force minimization, highlighting the effectiveness of the pole placement technique in seismic excitation scenarios. Zhou et al. [21], investigated the optimal sensor placement strategy for a cat-head-type transmission tower using the Effective Independence (EI) method, and proposed a novel technique for determining the minimum number of sensors necessary for structural health monitoring. The study identifies the optimal sensor count based on the lowest Modal Assurance Criterion (MAC) value, demonstrating that sensor configurations for larger sets naturally include those of smaller, optimal arrangements. Mei et al. [22], developed a genetic algorithm-based approach to optimize active control systems in civil structures subjected to random seismic excitations. This method concurrently optimizes both the number and placement of actuators, along with the control algorithm itself, while explicitly considering the stochastic nature of seismic events. The approach's effectiveness, efficiency, and stability were validated through two numerical case studies. Results indicated that the genetic algorithm demonstrated robust convergence behavior and stability, consistently achieving global or near-global optimal solutions across multiple independent simulations. Finally, Hamdaoui et al. [23], conduct a parametric study of the effect of varying the position of Shape Memory Alloy (SMA) devices used for the rehabilitation of historical structures to determine the optimal location. A 3D finite element model of a minaret was calibrated and validated based on experimental results from ambient vibration testing, followed by a nonlinear transient analysis under the influence of the El Centro earthquake. Various simulation scenarios, involving the placement, number, and type of (SMA) devices, were explored to observe their influence on the seismic response of the minaret, confirming the effectiveness of the proposed SMA device. In conclusion, an optimized arrangement of (SMA) allows for an effective mitigation of the seismic response, particularly at the stress level, with a limited number of wires.

This literature review reveals that the majority of past research has focused on determining a fixed number of actuators in control systems. This study aims to answer important questions about how to best place control systems and how this affects the way tall buildings behave, especially in areas that often experience earthquakes, due to the growing difficulties in civil engineering.

The study begins with a detailed review of the state of the art on structural optimization and active control. This is followed by the presentation of the proposed methodology and a dedicated strategy designed to address the research problem, including a description of the developed algorithm. A rigorous validation of the structural model is then carried out to ensure reliability. Once validated, the three proposed optimization methods for the optimal placement of control

systems are applied. An in-depth parametric study is subsequently conducted to evaluate the influence of key parameters on the system's performance. Finally, practical recommendations are provided to assist engineers and researchers in selecting and implementing optimized control solutions.

In this study, we investigate the integration of actuators in the active tendon system and its effect on reducing maximum structural displacement, in comparison to passive control approaches. While many previous works have employed genetic algorithms to identify optimal placement, our approach incorporates additional methods. In particular, the LQR algorithm is applied for active structural control.

The primary objective of this research is to develop a comprehensive framework that integrates advanced control systems - specifically active tendons- to enhance the seismic resilience of tall buildings. Leveraging state-of-the-art computational tools and optimization algorithms, including genetic algorithms, this study aims to provide actionable insights and guidelines for designing and implementing effective structural control strategies in earthquake-prone regions. An 11-story building model serves as the case study for testing the optimization of active tendon placement. Three distinct methods are applied to identify the most effective configurations of control systems. In addition, the structure is subjected to various seismic excitations to assess the robustness and efficiency of each approach. The analyses are conducted using the MATLAB toolbox, which enables the identification of optimal solutions through objective function minimization. This software provides enhanced flexibility, advanced customization options, and improved accuracy in time-domain analysis and vibration control.

The conclusion summarizes the main findings, offers practical recommendations, and out-lines potential directions for future research in the field of structural control under seismic loading.

2. Methodology and Mathematical Models

The practical implementation of basic analog models is designed to represent the dynamic response of a foundation interacting with the supporting soil [24]. These models are also used to study the behavior of both structures and soils [25]. The practical application of these analog models offers valuable insights [26, 27].

The dynamic equation for an n-story building, incorporating the active tendon at all levels, can be formulated into a matrix equation as follows:

$$M\ddot{X}(t) + C\dot{X}(t) + KX(t) = -M_e\ddot{x}_g(t) + \Gamma U(t) \quad (1)$$

where M, C, and K are the (n+2 × n+2)-dimensional matrix of mass, damping and stiffness, respectively. $\ddot{x}_g(t)$ is the ground acceleration vector and X(t) is the response vector expressed by:

$$X(t) = \{x_1, x_2, \dots, x_n, x_b, \varphi_y\}^{\mathrm{T}} \quad (2)$$

Also, $\dot{X}(t)$ represents the velocity and $\ddot{X}(t)$ represents the acceleration of the building's center of mass including both translational and rotational movements of the foundation. Γ is the matrix that indicates the location of the controllers, assuming active tendons are installed on every floor, with dimensions of (n+2 × n). U(t) is the vector that contains the active control forces acting horizontally, with dimensions of (n × 1). Based on these explanations, the matrix Γ can be written as:

$$\Gamma = [\,[\Gamma^*] \;\; ; \;\; [0]\,] \quad (3)$$

where [0] is a (2 × n) matrix filled with zeros to ensure that no direct control forces are applied to the rotational and translational movements of the foundation. [Γ*] is an (n × n) matrix that is defined as:

$$\Gamma^* = \begin{bmatrix} -1 & 1 & 0 & \cdots & 0 & 0 \\ 0 & -1 & 1 & \cdots & 0 & 0 \\ \cdots & \cdots & \cdots & \ddots & \cdots & \cdots \\ 0 & 0 & 0 & \cdots & -1 & 1 \\ 0 & 0 & 0 & \cdots & 0 & -1 \end{bmatrix} \quad (4)$$

The vector defines the horizontal aspect of the active control force as:

$$U(t) = \{u_1, u_2, \dots, u_n\}^{\mathrm{T}} \quad (5)$$

3. Active Control Strategy

Within control theory [28], the motion equation for a structure under active control, as presented in Equation 1, can be efficiently reformulated in state-space form as:

$$\dot{Z}(t) = AZ(t) + B_u U(t) + B_r\ddot{x}_g(t) \quad (6)$$

where, A represents a matrix of dimensions (2n+4 × 2n+4). Bu represents a vector with dimensions (2n+4 × n) and Br is a matrix with dimensions (2n+4 × 1). These can be de-scribed as follows:

$$A = \begin{bmatrix} 0 & I \\ -M^{-1}K & -M^{-1}C \end{bmatrix} \quad (7)$$

$$B_u = \begin{bmatrix} 0 \\ M^{-1}\Gamma \end{bmatrix} \quad (8)$$

$$B_r = \begin{bmatrix} 0 \\ -M^{-1}M_e \end{bmatrix} \quad (9)$$

Z(t) and $\dot{Z}$(t) are vectors each with dimensions of (2n+4 × 1):

$$Z(t) = \begin{bmatrix} X(t) \\ X(t) \end{bmatrix}; \dot{Z}(t) = \begin{bmatrix} X(t) \\ \ddot{X}(t) \end{bmatrix} \quad (10)$$

The control force U(t) is calculated by aiming to minimize the quadratic performance index J, as specified in Cheng et al. [28]:

$$J = \int_{t_0}^{t_f} \{Z(t)\}^T [Q] \{Z(t)\} + \{U(t)^T [R] \{U(t)\}) \, dt \quad (11)$$

where; t_0 and t_f represent the start and end times of the excitation, respectively.

The matrix Q with dimensions of (2n × 2n), is both semi-definite positive and symmetric. A positive-definite Q implies that all degrees of freedom are accounted for in the index J. However, if Q is semi-definite and has zero eigenvalues, it may exclude some degrees of freedom. R is a symmetric and positive-definite matrix with dimensions (r × r). Both Q and R serve as weighting matrices for the response and the control force, respectively.

$$Q = a \begin{bmatrix} K & 0 \\ 0 & M \end{bmatrix}; R = bI_p \quad (12)$$

where I_p is identity matrix, and a and b are the matrix coefficients of Q and R given in section 5.2, respectively. The performance index is designed to strike a balance between the structural response and the control energy, with the objective of minimizing the structure's response. The goal is to minimize both the structural response and control energy over the time interval from t_0 to t_f. High values in Q prioritize minimizing the system's response at the cost of increased control force, while high values in R reduce the control force but may fail to sufficiently decrease the structural response [22]. In Equations 1 and 6, the control force vector U(t) is dimensioned as (n × 1):

$$U(t) = -GZ(t) = -R^{-1}B_u{}^{\mathrm{T}}PZ(t) \quad (13)$$

where, G represents the gain matrix, and P is a matrix with dimensions (2n+4 × 2n+4), which is computed by resolving the nonlinear matrix equation known as RICCATI as shown Equation 14 [28]:

$$PA + A^{\mathrm{T}}P - PB_uR^{-1}B_u{}^{\mathrm{T}}P + Q = 0 \quad (14)$$

By integrating Equation 6 with Equation 14, the resultant Equation is as follows:

$$\dot{Z}(t) = AZ(t) + B_u(-R^{-1}B_u{}^{\mathrm{T}}PZ(t)) + B_r\ddot{x}_g(t) \quad (15)$$

Considering:

$$A^* = A - B_uR^{-1}B_u{}^{\mathrm{T}}P \quad (16)$$

Equation 15 can be expressed as:

$$\dot{Z}(t) = A^*Z(t) + B_r\ddot{x}_g(t) \quad (17)$$

To examine the structural response within the state-space framework, it's necessary to consider not only Equation 17 but also define Equation 18:

$$y = EZ(t) + L\ddot{x}_g(t) \quad (18)$$

where the matrices E and L are described as follows:

$$E = \begin{bmatrix} I & 0 \\ 0 & I \\ -M^{-1}K & -M^{-1}C \end{bmatrix}; L = \begin{bmatrix} 0 \\ B_r \end{bmatrix} \quad (19)$$

The procedure for computing the control force in an active control system can be summarized as follows:

- First, define the weighting matrices Q and R.
- Next, solve the algebraic RICCATI equation using the system matrices A and B_u, in conjunction with the defined weighting matrices Q and R.
- Then, determine the gain matrix G, which is subsequently used to calculate the control force U(t).

The Figure 1 illustrates a typical three-dimensional structural system reinforced by active tendons. This simplified model represents a floor of a building subjected to bidirectional seismic forces. The device relies on the installation of diagonal cables (tensioners) whose tension is actively modulated by strategically placed actuators. These actuators are controlled by a control algorithm based on the structural response measurements (displacements, velocities, accelerations), thus enabling active vibration reduction.

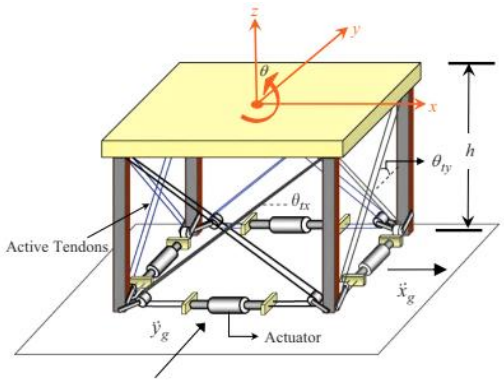

Figure 1. Typical story with active tendon control devices

4. Methods for Choosing the Optimal Position of Control Systems

4.1. Formulating the Optimization Challenge

Optimization theory has become an essential tool in engineering design, enabling the identification of optimal solutions through the formal definition of an optimization problem. Such problems involve maximizing or minimizing an objective function that serves as the optimization criterion. In the context of smart structures, the optimal placement of control devices is particularly critical, as these devices regulate structural behavior by applying control forces via actuators. To effectively reduce seismic responses, these forces must be comparable in magnitude to the inherent damping forces of the structure. Nevertheless, the overall cost of control systems can be reduced by strategically positioning them to enhance their effectiveness [28]. The primary goal of optimizing control device placement is, therefore, to achieve a significant reduction in seismic structural response while minimizing the amount of control force required. Therefore, the overarching optimization problem can be formulated as follows [16]:

$$\begin{cases} Minimize: \{f(x)\} \\ Subject\ to: g(x) = g_0\ ;\ 1 \le x \le N \end{cases} \quad (20)$$

In this context, the function f(x) represents the optimization objective. For control device optimization, f(x) may correspond to the structural response in passive systems, the control force in active systems or a weighted combination of active and passive control forces in hybrid systems. The function g(x) defines the control objective, which may not be applicable to passive systems but is typically associated with structural displacement, velocity, or inter-story drift in active or hybrid systems. Here, g_0 denotes the target structural response level to be achieved through control. The variable (x) denotes a design parameter—such as the story level at which a control device is installed in a single-bay multi-story building—with N representing the total number of stories. When multiple control devices are employed within a seismic response control system, (x) becomes a vector, where each element specifies the placement of an individual control device.

4.2. The Modal Controllability Method

This method relies on the modal properties of the structure to determine the optimal positions for control devices. It is particularly useful for providing an initial approximation, especially in structures where modal response dominates. However, it may not fully capture the dynamics of complex structures or those subjected to non-modal dynamic loads [28]. Through modal analysis of the system, we obtain:

$$\{X(t)\} = [\phi]\{q(t)\} \quad (21)$$

By replacing Equation 21 in Equation 1, we will obtain:

$$[M^*]\{\ddot{q}(t)\} + [C^*]\{\dot{q}(t)\} + [K^*]\{q(t)\} = [\phi]^T [\gamma] \{U(t)\} + [\phi]^T \{\delta\} \ddot{x}_g(t) \quad (22)$$

where M*, C*, K* are the diagonal matrices of mass, damping and stiffness, respectively, and ϕ and q(t) represent the matrix of modal shapes and the modal coordinate vector, respectively. By dividing by the mass term, the modal equation for each value of "i" (where i = (1 …n), "n" is the number of (DOF) is given by:

$$\ddot{q}_i(t) + 2\xi_i w_i \dot{q}(t) + w_i^2 q_i(t) = \gamma_i U(t) + \delta_i \ddot{x}_g(t) \quad (23)$$

The representation of Equation 23 in terms of the state variables is as follows:

$$\begin{Bmatrix} \dot{q}(t) \\ \ddot{q}(t) \end{Bmatrix} = \begin{bmatrix} 0 & 1 \\ -w_i{}^2 & -2\xi_i w_i \end{bmatrix} \begin{Bmatrix} q(t) \\ \dot{q}(t) \end{Bmatrix} + \begin{bmatrix} 0 \\ \gamma_i \end{bmatrix} \{U(t)\} + \begin{Bmatrix} 0 \\ \delta_i \end{Bmatrix} \ddot{x}_g(t) \quad (24)$$

The approach outlined in Equation 24 is one of the strategies for determining the optimal placement of an active tendon within a given structure. Using the same model, we will implement active control with multiple ATs to identify the most effective floor for optimal placement:

$$\{\delta_i^j\} = \{\phi_i\}^T \{\gamma\}_j \quad (25)$$

where "i" represents the total Eigen mode, "j" is a floor count, $\{\delta_i^j\}$ is the modal controllability vector, $\{\phi_i\}^T$ is an Eigen mode, and $\{\gamma\}_j$ denotes the vector indicating where the AT control force is applied on the i^{th} floor. Therefore, the effectiveness of the control force is directly related to the absolute value of $\{\gamma\}_j$, making it a crucial metric for assessing modal controllability. The optimal placement of active tendons occurs where $\{\gamma\}_j$ reaches its highest absolute value.

4.3. Controllability Index

This index measures the ease of controlling a structure from a specific position. It incorporates more detailed aspects of the system than modal controllability, allowing for a more precise analysis of specific structures. However, its calculation can be more complex and may require a deeper understanding of the structure. In an AT control system, the controllability index is defined as [28]:

$$\rho(x) = max \sqrt{\sum_{j=1}^{n} \{\frac{\Delta [\emptyset j(x)]}{\Delta x} Y_j(t)\}^2} \quad (26)$$

where (x) is a percentage of the total height of the structure at the actuator location with $0 \leq x \leq 1$; "n" is the number of significant modes; $\emptyset_j(x)$ is the mode shape at position x; Y_j is the maximum value of the response spectrum for the j^{th} mode; and Δ refers to the spatial difference of the quantity from position x_1 to position x_2, where x_1 is the height ay which the actuating cylinder is attached, and x_2 is the height where the tendon is anchored. Δx is the height difference between x_1 and x_2. The optimal location is defined as the value of x for which ρ(x) is maximized. The next best location for the actuator corresponds to the value of x where ρ(x) is the second-largest value, and so on.

The effect of seismic excitations is typically characterized by the peak value of the response spectrum. One advantage of employing the controllability index as a criterion lies in its simplicity, as it provides a clear and easily defined objective function while allowing the simultaneous consideration of multiple significant vibration modes. However, this method is based solely on the response spectra and mode shapes of the uncontrolled structure, which can limit its accuracy and reduce its suitability for more complex or controlled structural systems.

4.4. Genetic Algorithm

Genetic algorithms (GAs) are optimization methods inspired by the principles of natural evolution. They are highly flexible and can be applied to optimize various aspects of a control system, such as the placement and number of devices. While powerful, GAs requires careful selection of algorithm parameters and can demand significant computational resources.

GA is particularly effective for problems where:

- There are a very large number of potentially good solutions.
- There is no deterministic algorithm to calculate the best solution(s).
- The problem space is not fully formalized.

The core of a genetic algorithm involves applying evolutionary principles to an optimization problem.

Unlike traditional algorithms, GAs begins with a population of starting points rather than just one. Various mechanisms allow the exploration of the solution space, making it possible to find an optimal or near-optimal solution.

Although there is no certainty of achieving the absolute best solution, the search space explored by GAs is typically much larger than that of traditional algorithms [29, 30]. In summary, the genetic algorithm operates as follows:

```
t = 0;
Initialize Population (P(t = 0));
Evaluate Population (P(t = 0));
while (not Terminated) do
{ Select Parents;
Reproduce Offspring;
Apply Mutation;
Perform Crossover;
Evaluate Population;
P(t + 1) = Create Next Generation from
P(t);
 t = t + 1; }
end
```

The goal of the multi-objective function is to minimize both the displacement of the top story and the number of stories equipped with active tendons. The presence of active tendons in a given story is represented by a binary indicator, where a value of 1 signifies the presence of an active tendon, and zero indicates its absence. There are two main objectives:

- 1st: Minimize the total number of active tendons across all stories, representing the extent of active control implemented throughout the building.
- 2nd: Assess the effectiveness of the active control system by comparing the base control force in the building with active tendons to that in a scenario where no active controls are applied.

Genetic Algorithms distinguish themselves from traditional optimization techniques commonly used in engineering design by several key characteristics. These distinctions are summarized in Table 1.

Table 1. Comparing genetic algorithms to other optimization techniques

	Genetic Algorithms	Other Optimization Techniques
Variables	Operate using a coded set of variables	Directly manipulate the variables
Searching method	Utilizes a population of potential solutions	Focuses on optimizing a single solution
Risk of converging to a local optimum	Low	High
Type of information used	Based on objective function values	Relies on gradient information
Rule types	Rules based on probabilities	Fixed, Unchanging rules

5. Numerical Studies

5.1. Developed Program

Based on the theoretical framework, a numerical simulation was conducted using MATLAB (Figure 2), where a program was developed to analyze the dynamic behavior of structures (beam-column types). The program is capable of studying structures with any number of floors and control systems, optimizing the placement of control devices using the three methods described earlier. It can handle both cases with or without control systems.

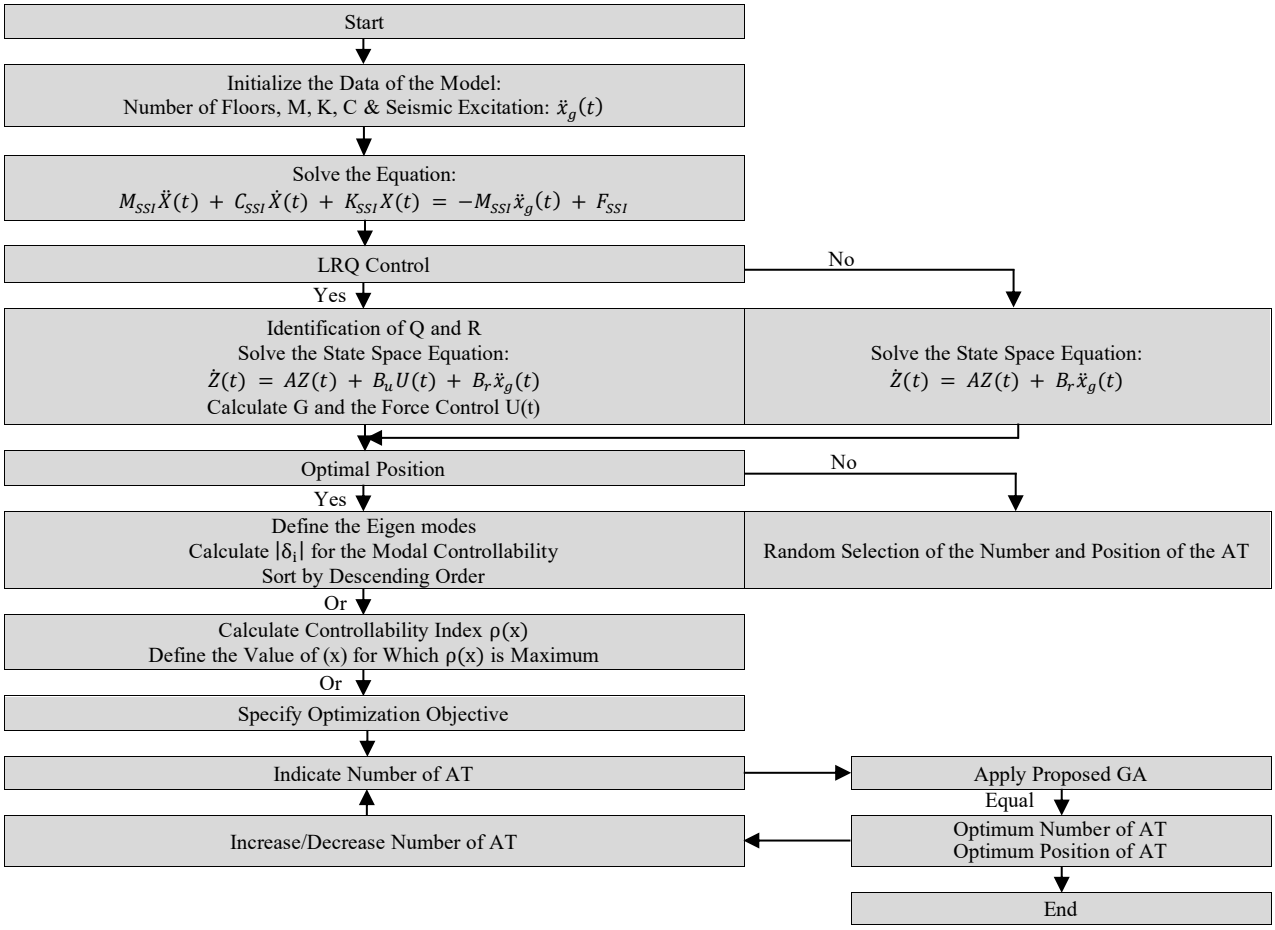

Figure 2. Simulation modeling process

5.2. Validation of the Case Study

This study focuses on an 11-story building modeled as a shear frame, with the problem formulated in the state space. The structural properties, listed in Table 2, are derived from the case study presented in Pourzeynali et al. [11]. For validation, we use data from Pourzeynali et al. [11], which describe the same 11-story shear frame building. This validation incorporates both the structural characteristics and the control systems, including TMD and Active TMD with LQR control strategies.

Table 2. Structural input of the 11-story building

Floors	Mass (kg)	Floors	Stiffness (N/m)
1	2.15e05	1	4.68e08
2-3	2.01e05	2	4.76e08
4	2.00e05	3	4.68e08
5-7	2.01e05	4-7	4.50e08
8-10	2.03e05	8-10	4.37e08
11	1.76e05	11	3.12e08

Regarding Q and R, their values are defined in Pourzeynali et al. [11]:

$$R = 1.5 \times 10^{-4} I_p;\ Q = a\begin{bmatrix} Q_{11} & 0 \\ 0 & Q_{22} \end{bmatrix} \tag{27}$$

$$\begin{cases} Q_{11} = 0.1 \times diag(ones(1,9), 0.15, 0.005) \\ Q_{22} = 0.001 \times diag(ones(1,9), 0.15, 0.005) \end{cases} \tag{28}$$

I_p is Identity matrix (2n+4 × 2n+4).

The a value for the 11-story buildings is set at 10^5. The results show a decrease in the horizontal force exerted by the active tendons as we move from the first to the last floor, with the highest force applied at the first floor. The system's damping ratio is: ξ=7% and the mass of the TMD is:

$$m_{TMD}/M_{\text{structure total mass}} = 3\% \tag{29}$$

These control systems are used to compare displacement results. Our findings are validated and compared in Tables 3 and 4, where identical structural properties are applied in simulations for the El Centro and Northridge earthquake scenarios. The analysis of the results revealed variations ranging from 0% to 9%, indicating a strong correlation and minimal error with the values presented in Pourzeynali et al. [11]. This comparison, shown in both tables, justifies the choice of the model used in this study. It is important to note that the control system considered here is solely the active tendon, with the control force being calculated using the (LQR) approach. Additionally, the reduction ratio is influenced by the selected excitation, and this study examines two earthquake records, as shown in Figure 3. The various scenarios analyzed are summarized in Table 5.

Table 3. Comparison of the effect of different controller systems for El Centro earthquake

Floors	Pourzeynali et al. [11]			Present study			Error %		
	Maximum uncontrolled response (m)	Controlled to uncontrolled response ratio (reduction ratio)		Maximum uncontrolled response (m)	Controlled to uncontrolled response ratio (reduction ratio)				
		TMD	ATMD (LQR)		TMD	ATMD (LQR)	Uncontrolled response	TMD	ATMD
1	0.019	0.68	0.49	0.020	0.66	0.50	5.26	2.94	2.04
2	0.039	0.64	0.46	0.040	0.63	0.50	2.56	1.56	8.69
3	0.057	0.65	0.47	0.059	0.65	0.49	3.50	0.00	425
4	0.074	0.65	0.47	0.074	0.66	0.48	0.00	1.53	2.12
5	0.09	0.64	0.48	0.09	0.66	0.48	0.00	3.12	0.00
6	0.10	0.67	0.50	0.10	0.69	0.50	0.00	2.98	0.00
7	0.12	0.62	0.48	0.115	0.63	0.50	4.16	1.61	4.16
8	0.13	0.64	0.46	0.12	0.65	0.48	7.69	1.56	4.34
9	0.14	0.67	0.48	0.13	0.67	0.51	7.14	0.00	6.25
10	0.14	0.67	0.50	0.14	0.67	0.50	0.00	0.00	0.00
11	0.147	0.673	0.49	0.145	0.678	0.48	1.36	0.74	2.04

Table 4. Comparison of the effect of different controller systems for Northridge earthquake

Floors	Pourzeynali et al. [11]			Present study			Error %		
	Maximum uncontrolled response (m)	Controlled to uncontrolled response ratio (reduction ratio)		Maximum uncontrolled response (m)	Controlled to uncontrolled response ratio (reduction ratio)				
		TMD	ATMD (LQR)		TMD	ATMD (LQR)	Uncontrolled response	TMD	ATMD
1	0.046	0.86	0.72	0.045	0.90	0.75	2.17	4.65	4.16
2	0.088	0.91	0.72	0.085	0.91	0.75	3.40	0.00	4.16
3	0.123	0.89	0.89	0.121	0.90	0.90	1.62	1.12	1.12
4	0.15	0.93	0.73	0.148	0.90	0.80	1.33	3.22	9.58
5	0.18	0.89	0.72	0.179	0.93	0.78	0.55	4.49	8.33
6	0.194	0.92	0.77	0.192	0.90	0.77	1.03	2.17	0.00
7	0.204	0.93	0.83	0.200	0.91	0.84	1.96	2.15	1.20
8	0.210	0.95	0.86	0.210	0.94	0.85	0.00	1.05	1.16
9	0.22	1.00	0.86	0.22	0.98	0.86	0.00	2.00	0.00
10	0.23	1.00	0.91	0.23	0.98	0.91	0.00	2.00	0.00
11	0.23	1.00	0.95	0.23	1.00	0.95	0.00	0.00	0.00

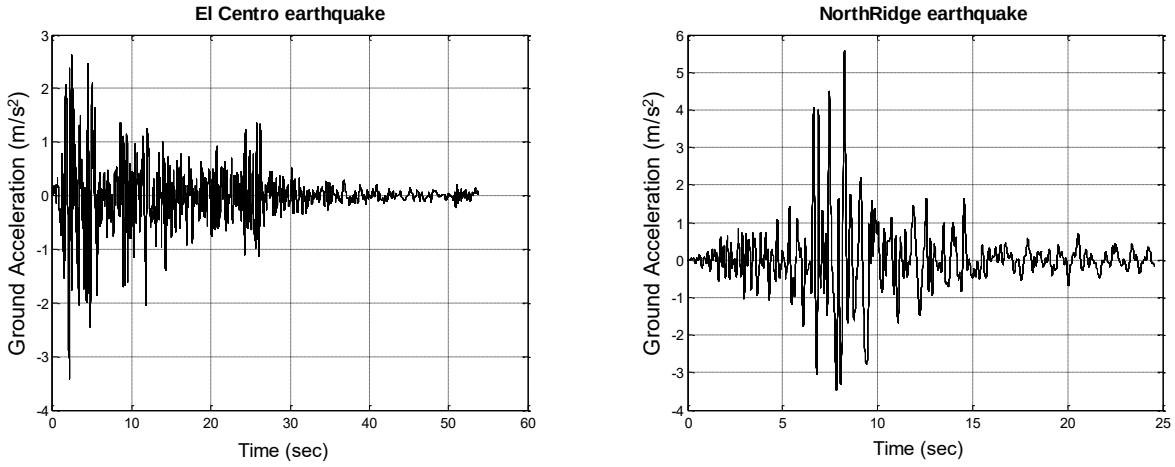

(a) (b)

Figure 3. The earthquake for applying to the structure: (a) El Centro; (b) Northridge

Table 5. Optimal position according to the response spectrum

El Centro spectra ρ	1.465	1.430	1.364	1.352	1.198	0.995	0.993	0.804	0.607	0.380	0.372
Optimal position (Floors)	4	5	3	6	7	2	8	9	10	1	11
Northridge spectra ρ	1.697	1.630	1.542	1.535	1.532	1.47	1.362	1.337	1.042	0.615	0.547
Optimal position (Floors)	3	4	5	6	7	8	2	9	10	11	1

5.3. Application of Modal Controllability

It is observed that each mode suggests a unique optimal placement for the active tendon. While this approach is straightforward to implement and independent of the earthquake type, it has a significant limitation. Its effectiveness is primarily restricted to structures dominated by a single mode, which is rarely the case with smart structures that typically exhibit multiple significant modes. Therefore, the optimal placement of ATs corresponds to the location with the maximum absolute value of the modal controllability $|\delta_i^j|$, as shown in Equation 25. For instance, as illustrated in Figure 4 and detailed in Table 6, the first three modes are the most dominant for the structure in this study.

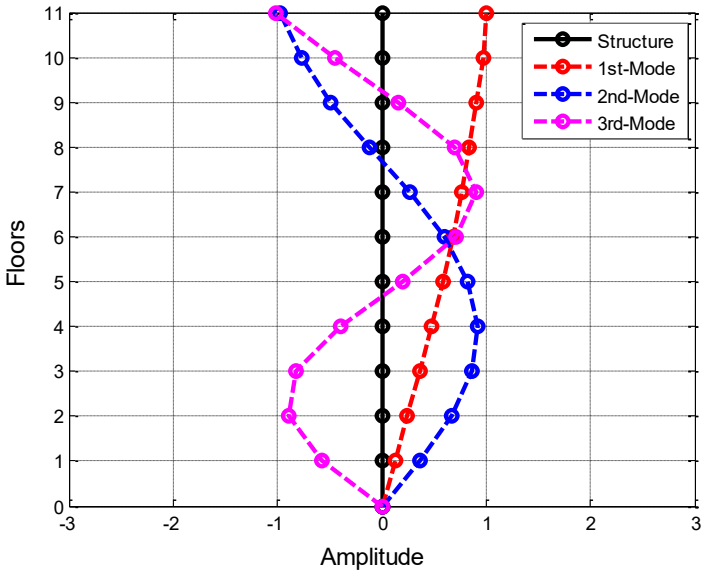

Figure 4. Dominant Eigen modes

Table 6. Optimal position according to the dominant Eigen modes

1st mode $\|\delta_1\|$	0.125	0.120	0.118	0.115	0.107	0.095	0.082	0.070	0.052	0.034	0.023
Optimal position (Floors)	1	2	3	4	5	6	7	8	9	10	11
2nd mode $\|\delta_2\|$	0.387	0.366	0.366	0.331	0.298	0.281	0.232	0.206	0.196	0.093	0.060
Optimal position (Floors)	8	1	9	7	2	10	6	11	3	5	4
3rd mode $\|\delta_3\|$	0.608	0.602	0.576	0.565	0.535	0.510	0.428	0.310	0.215	0.193	0.062
Optimal position (Floors)	10	5	1	11	9	6	4	2	8	7	3

The graphical representation of modal controllability values in Figure 5 clearly shows that the optimal placement of active tendons depends on the shape of each mode of the structure, corresponding to its maximum modal controllability |δ|. In Table 6, we investigate the effect of varying the number of ATs by positioning them optimally according to the 1st mode. With the application of the two seismic signals plotted in the Figure 3.

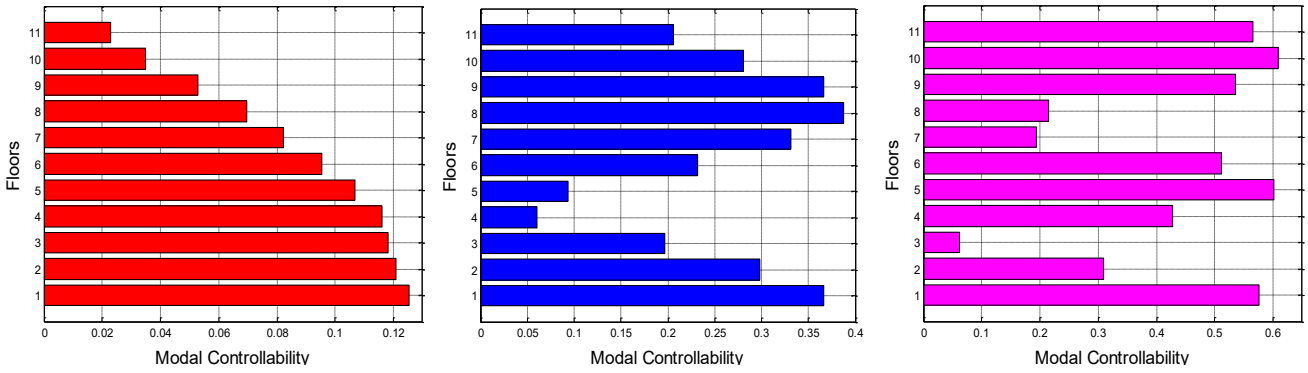

Figure 5. Modal controllability values for optimal actuator locations: (a) 1st mode; (b) 2nd mode; (c) 3rd mode

From the data presented in Table 7 and illustrated in Figure 6, it is evident that placing the AT in the lower half of the building results in a significant reduction in maximum displacement. When evaluating different configurations of AT placement—comparing 1 AT, 3 ATs, 5 ATs, and full-floor control—the displacement reductions are as follows: 3.45%, 8.28%, 17.24%, and 21.37% for the El Centro earthquake, and 2.60%, 6.10%, 11.74%, and 15.22% for the Northridge earthquake.

Table 7. Comparison of the effect of the different numbers of AT with their optimal position

Building floors	El Centro earthquake					Northridge earthquake				
	Max uncontrolled response (m) Fixed-Base	Max controlled response (m) Fixed-Base				Max uncontrolled response (m) Fixed-Base	Max controlled response (m) Fixed-Base			
		1 AT	3 AT	5 AT	All floors		1 AT	3 AT	5 AT	All floors
1	0.020	0.019	0.018	0.016	0.012	0.045	0.044	0.038	0.030	0.026
2	0.040	0.039	0.038	0.036	0.030	0.085	0.084	0.075	0.061	0.052
3	0.059	0.058	0.057	0.050	0.045	0.121	0.12	0.11	0.090	0.080
4	0.074	0.073	0.072	0.064	0.058	0.148	0.146	0.132	0.113	0.102
5	0.09	0.089	0.084	0.077	0.072	0.179	0.176	0.16	0.141	0.13
6	0.10	0.098	0.096	0.088	0.082	0.192	0.19	0.18	0.158	0.146
7	0.115	0.112	0.108	0.099	0.091	0.200	0.198	0.19	0.175	0.163
8	0.12	0.119	0.115	0.108	0.099	0.210	0.207	0.197	0.183	0.172
9	0.13	0.128	0.124	0.114	0.107	0.22	0.216	0.208	0.196	0.188
10	0.14	0.136	0.130	0.119	0.112	0.23	0.223	0.215	0.202	0.194
11	0.145	0.140	0.133	0.120	0.114	0.23	0.224	0.216	0.203	0.195

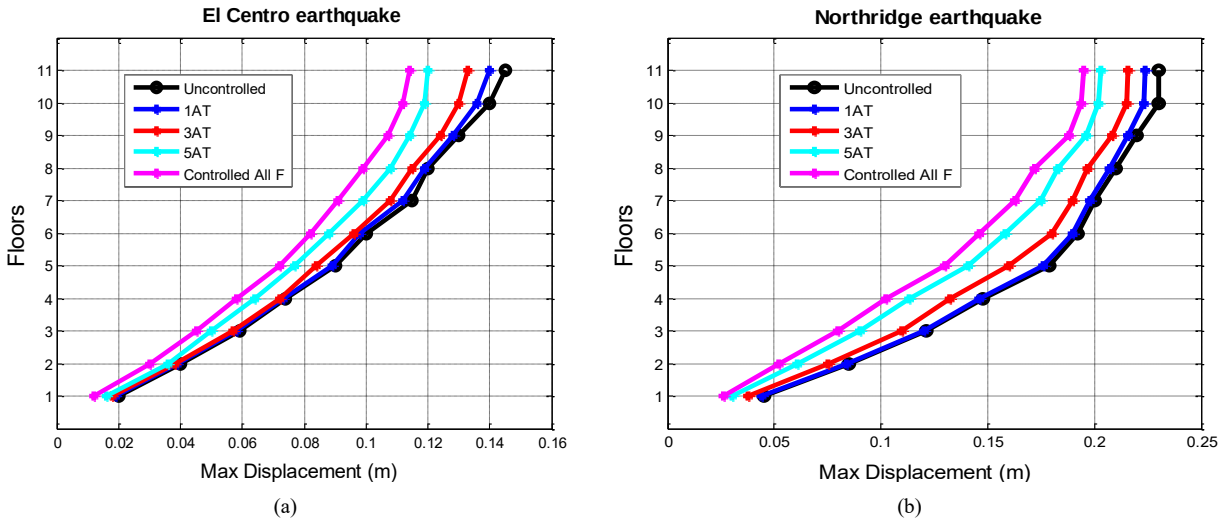

Figure 6. Comparison of max displacement response: (a) El Centro; (b) Northridge

These results indicate that while increasing the number of ATs leads to a reduction in displacement, the benefits from adding more than half of the floors are marginal, with less than a 4% difference for both earthquakes

5.4. Application of Controllability Index

The criteria for actuator placement are developed under the following assumptions:

- The influence of each vibration mode is evaluated using the mode shapes of the structure in its uncontrolled state.
- The structural response is assessed under actual seismic excitations by employing the response spectra of the El Centro and Northridge earthquakes to analyze the behavior of the structure without control mechanisms.
- Active control systems are implemented using Active Tendons (ATs), where the actuators are modeled as linear devices with proportional control behavior.
- The effectiveness of the ATs is assumed to be uniform across all building stories, thereby facilitating a consistent evaluation of their impact on overall structural performance.

For analytical purposes, ATs are initially placed at the ground floor, assuming uniform story heights throughout the building. The natural frequencies of the structure are determined as follows:

$$f_i = \omega_i / 2\pi \tag{30}$$

Using the Pseudo-Velocity response spectrum for the El Centro and Northridge earthquakes, shown in Figure 7 with a damping ratio of ξ=5%, the maximum values of the modal response, can be obtained as follows:

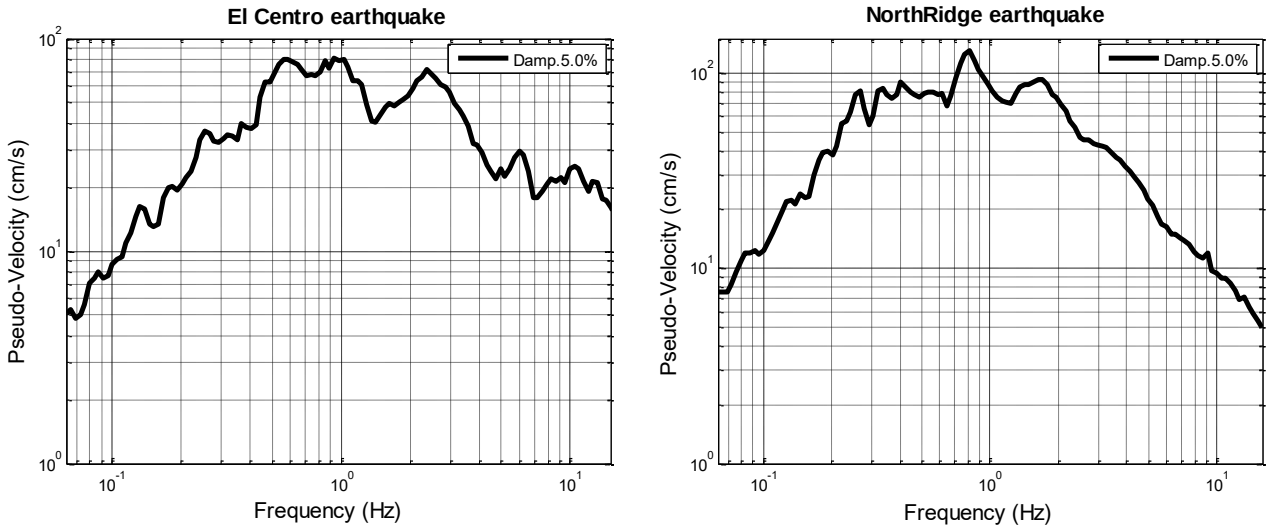

(a) (b)

Figure 7. Response spectrum: (a) El Centro; (b) Northridge

Given that all floors of the structure are equal height with $\Delta x = 0.6$, the controllability index is influenced by the response spectra of the earthquake. By calculating the highest controllability index, as defined in Equation 26, for both the El Centro and Northridge spectra, the optimal placement for the active tendon can be determined.

The values of the controllability index $\rho(x)$ for each potential tendon location are presented in Table 5, and a graphical representation is shown in Figure 8. The data indicate that the optimal actuator locations, based on the controllability index, are situated on the lower floors for both earthquake scenarios.

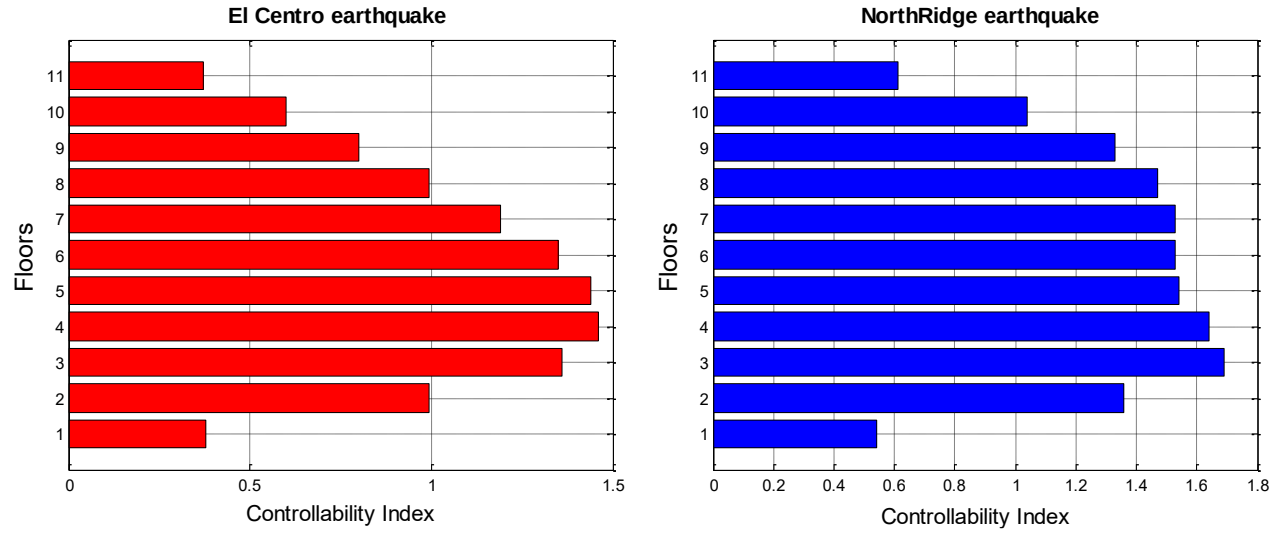

(a) (b)

Figure 8. Controllability index values for optimal actuator locations: (a) El Centro; (b) Northridge

A higher index value at a given location suggests that the control at the floor is likely to be more effective. Therefore, the results imply that control strategies may be more efficient when applied to lower floors, rather than higher levels, for the seismic profiles considered in this study. Specifically, the five largest values of $\rho(x)$ are found between the third and seventh floors when deploying 5ATs under both earthquake scenarios, identifying these as the optimal locations for the active tendons according to the controllability index criterion.

Following this, we implemented these optimal tendon positions and varied the number of ATs. The results of these changes are presented in Table 8 and illustrated in Figure 9.

Table 8. Effectiveness comparison of varying numbers of AT in optimal positions

Building floors	El Centro earthquake					Northridge earthquake				
	Max uncontrolled response (m) Fixed-Base	Max controlled response (m) Fixed-Base				Max uncontrolled response (m) Fixed-Base	Max controlled response (m) Fixed-Base			
		1 AT	3 AT	5 AT	All floors		1 AT	3 AT	5 AT	All floors
1	0.020	0.020	0.020	0.018	0.012	0.045	0.045	0.040	0.037	0.026
2	0.040	0.040	0.040	0.039	0.030	0.085	0.084	0.077	0.072	0.052
3	0.059	0.056	0.055	0.052	0.045	0.121	0.118	0.113	0.105	0.080
4	0.074	0.072	0.069	0.064	0.058	0.148	0.144	0.135	0.129	0.102
5	0.09	0.088	0.082	0.079	0.072	0.179	0.175	0.164	0.154	0.13
6	0.10	0.097	0.094	0.091	0.082	0.192	0.190	0.186	0.175	0.146
7	0.115	0.113	0.106	0.103	0.091	0.200	0.202	0.196	0.188	0.163
8	0.12	0.120	0.114	0.111	0.099	0.210	0.210	0.204	0.195	0.172
9	0.13	0.129	0.124	0.121	0.107	0.22	0.220	0.212	0.205	0.188
10	0.14	0.137	0.131	0.128	0.112	0.23	0.228	0.220	0.213	0.194
11	0.145	0.143	0.136	0.132	0.114	0.23	0.230	0.222	0.215	0.195

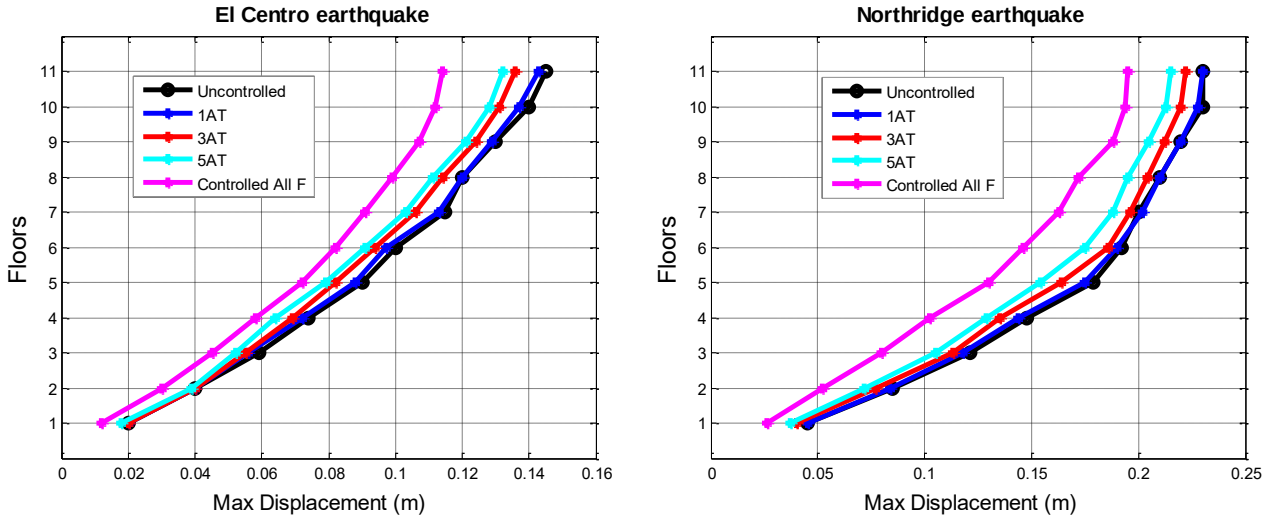

Figure 9. Comparison of max displacement response: (a) El Centro; (b) Northridge

Table 8 and its corresponding graphical representation in Figure 9 show that the actuator positions identified using the controllability index do not outperform those previously determined by modal controllability in terms of reducing displacements across the building's floors. This highlights the significance of employing multiple methods for determining the optimal placement of ATs. The numerical results clearly demonstrate the differences in displacement reductions between the two methods: 1.38%, 6%, and 9% for the 1 AT, 3 AT, and 5 AT configurations, respectively, under the El Centro earthquake. Similarly, for the Northridge earthquake, the differences are 0%, 4.35%, and 6.52% for the 1 AT, 3 AT, and 5 AT configurations, respectively.

These findings suggest that the actuator positions determined through modal controllability are more effective than those derived from the controllability index in terms of the reduction ratio.

5.5. Application of Genetic Algorithm

The benefit of this method lies in its ability to determine the optimal placement for any control system, whether passive or active. By optimizing the control force, the system can achieve the best placement for the actuators, thereby minimizing the maximum displacement of the structure.

A key advantage of this approach is that it does not require control at every level of the structure to achieve optimal results. Instead, the number of active tendons installed can be minimized while still ensuring effective control. The primary goal is to reduce the structural response with the least amount of control force.

In Table 9, it is observed that the optimal placements for varying numbers of ATs, as determined by the modal controllability method for the dominant mode, are also identified through the use of a genetic algorithm. Which is illustrated by Figure 10.

Table 9. Optimal position for choosing number of AT by GA for different cases considered

Scenarios	Number of AT	Optimal positions (Floor)	Maximum Controlled response (m)	Reduction ratio	Maximum Uncontrolled response (m)
1	1 AT	1	0.14	0.96	0.145
	3 AT	1 2 3	0.133	0.91	
	5 AT	1 2 3 4 5	0.12	0.82	
2	1 AT	1	0.224	0.97	0.23
	3 AT	1 2 3	0.216	0.93	
	5 AT	1 2 3 4 5	0.203	0.88	

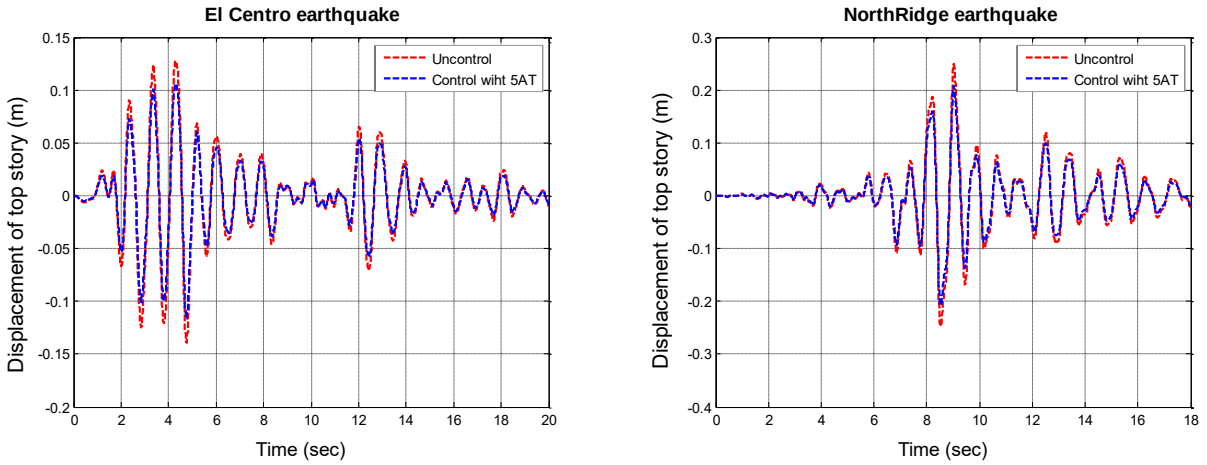

(a) (b)

Figure 10. Comparison of max displacement of top story using 5AT in their optimal placement using GA: (a) El Centro; (b) Northridge

All the results for the 11-story structure are summarized in Figure 11, providing a comparison of the three methods used to determine the optimal positions of the AT under the two seismic excitations considered. For the El Centro earthquake, the maximum floor displacements obtained through modal controllability and the genetic algorithm were identical, leading to a significant reduction of approximately 17.27%.

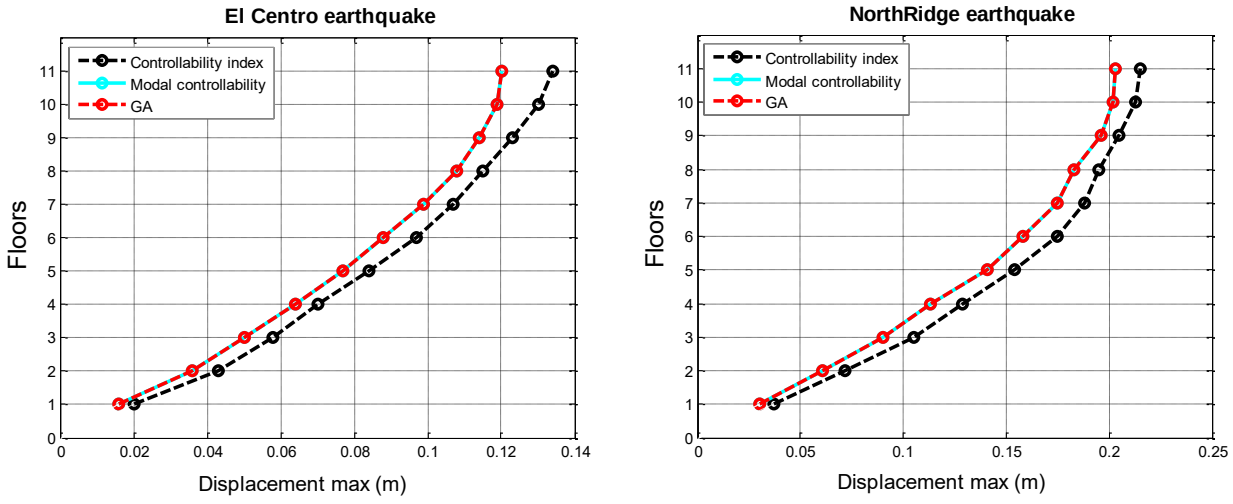

(a) (b)

Figure 11. Comparison of max displacement controlled response of stories with 5AT of all optimization methods: (a) El Centro; (b) Northridge

Additionally, the controllability index shows a reduction of 8.96% when compared to an uncontrolled structure. For the Northridge earthquake, the reductions in maximum floor displacements are identical across the three optimization methods, achieving a reduction of 11.74% with both modal controllability and genetic algorithm. In contrast, the controllability index results in a reduction of 6.52%.

In the second part of this study, we aim to examine the effects of varying the earthquake excitation and the number/type of the control system on their optimal placement and the corresponding reduction rates in displacement

control. By leveraging the advantages of the GA, which identifies the optimal locations for any control system, we seek to incorporate a cost criterion. This will allow us to determine the three optimal positions for each system—3 AT, 3 TMD, and 3 ATMD—under different earthquake scenarios.

Were used as external stimuli for the 11-story building equipped with various control systems. This setup was selected to identify the optimal placement of control devices and to investigate how these optimal positions change across the structure. Table 10 shows that the optimal placements for AT across eleven earthquakes generally fall between the 1st and 3rd floors, except the Kobe and Landers earthquakes, where they remain in the lower half of the building. For TMD, the optimal placement is always on the top floor. When a second TMD is introduced, the optimal positions range from the 10th to the 1st floor. In the case of ATMD, the best location is consistently the top floor for all earthquakes, with positions shifting to the 10th/1st or 3rd floor when an additional ATMD is added.

Table 10. Optimal position for 3AT, 3TMD and 3ATMD under different earthquakes

Earthquake name	Max Uncontrolled response (m)	Optimal position AT (Floors)			Reduction ratio	Optimal position TMD (Floors)			Reduction ratio	Optimal position ATMD (Floors)			Reduction ratio
El Centro	0.145	1	2	3	0.91	1	10	11	0.62	1	10	11	0.42
Northridge	0.230	1	2	3	0.93	1	10	11	0.90	1	10	11	0.86
Kobe	0.504	2	4	5	0.89	3	10	11	0.80	3	10	11	0.73
Chi-Chi	0.231	1	2	3	0.85	1	10	11	0.78	1	10	11	0.62
Loma-Prieta	0.123	1	2	3	0.94	1	9	11	0.89	1	10	11	0.79
Imperial Valley	0.282	1	2	3	0.85	1	8	11	0.75	1	10	11	0.58
Hollister	0.190	1	2	3	0.73	2	9	11	0.67	2	9	11	0.51
Kocaeli	0.161	1	2	3	0.78	2	10	11	0.72	1	10	11	0.55
Trinidad	0.121	1	2	3	0.80	1	10	11	0.70	1	10	11	0.48
Landers	0.113	1	3	4	0.82	3	10	11	0.87	3	10	11	0.59
Friuli	0.100	1	2	3	0.83	1	10	11	0.77	1	10	11	0.67

This variation in seismic signals illustrates that control systems often maintain their optimal positioning within the structure. To better visualize the results presented in Table 10, Figure 12 illustrates the distribution curve for various control systems across different earthquakes. It is highly recommended (with a 100% certainty) to install the first control system on the 1st floor for AT and on the 11th floor for both TMD and ATMD.

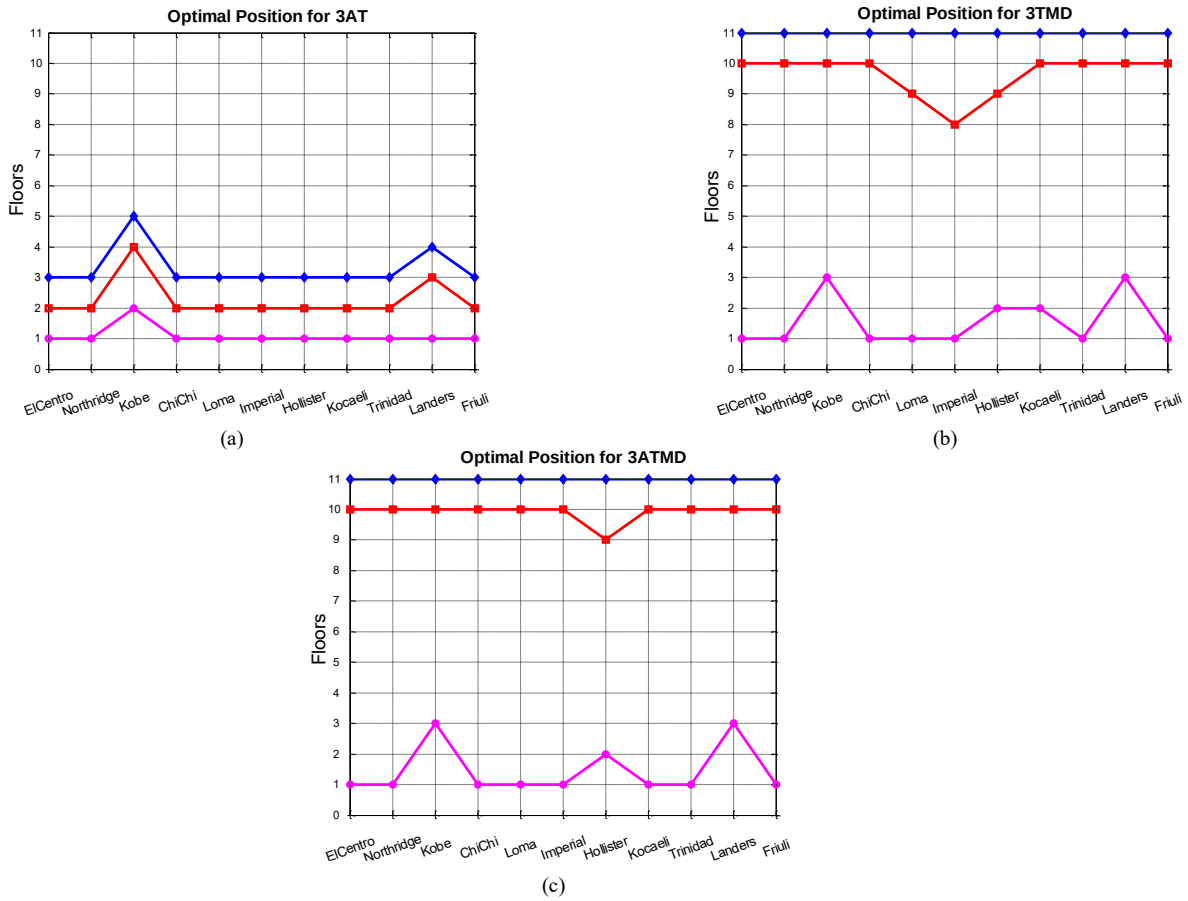

Figure 12. Optimal position for the three control systems under different earthquakes: (a) 3AT; (b) 3TMD; (c) 3ATMD

For approximately two-thirds of the scenarios, the second control system should be placed on the 2nd floor for AT and on the 10th floor for TMD and ATMD. The third control system is typically recommended for the 3rd floor when using AT and for the 1st floor in the case of TMD and ATMD, reflecting one-third of the results. As such, for this study, the 4th/5th floors for AT and the 9th/8th floors for TMD and ATMD are also considered optimal placement options.

The findings suggest that the optimization criteria, focused on minimizing peak displacement through a GA, favor specific floors for the installation of control systems, whether they are ATs, TMDs, or ATMDs. Figure 13 illustrates the placement of these systems, comparing arbitrary placements (top and bottom) with the optimal positions within an 11-story building. These placements are evaluated based on their impact on controlled displacements during various earthquakes, providing a basis for comparative analysis. This part of the study highlights that the effectiveness of the building's control can be greatly enhanced by strategically positioning control systems, rather than installing them indiscriminately at the highest or lowest points of the building.

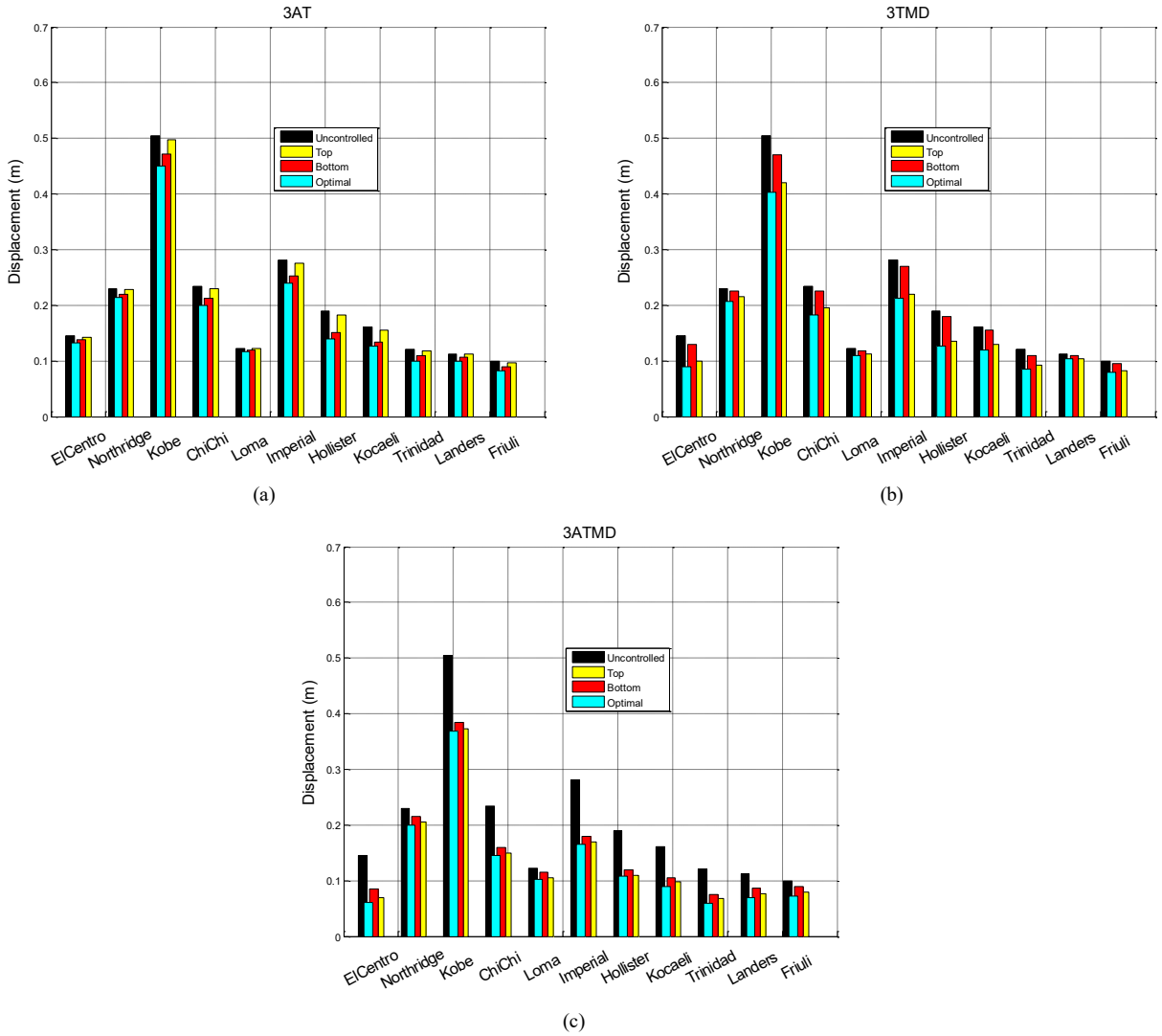

Figure 13. Performance of optimal position for the three control systems under different earthquakes using GA: (a) 3AT; (b) 3TMD; (c) 3ATMD

The optimization process is designed to stop once predefined criteria are achieved. Figure 14 illustrates this optimization journey for our study, highlighting how the system evolves over time. Table 11 lists the point at which peak performance, or "maximum fitness", is reached for various earthquakes. This is important because it shows the effectiveness of the optimization process in adapting to different seismic events. In Figure 14, we see two key lines: one for "Max Fitness" and another for "Mean Fitness" across generations. The "Max Fitness" line quickly rises to its highest level, indicating that the optimization process swiftly finds a good solution. The "Mean Fitness" line shows less variation over time, which suggests that, on average, the solutions are converging towards better fitness as the process evolves.

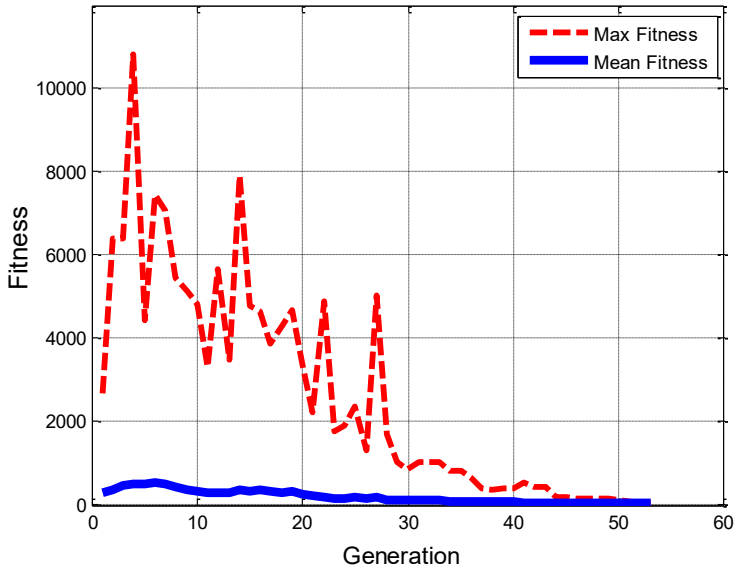

Figure 14. Evolution of fitness over generation during El Centro earthquake excitation for 3AT

Table 11. Generation achieving peak fitness across diverse earthquakes

Earthquake records	Generation achieving peak fitness
El Centro	55th generation
Northridge	80th generation
Kobe	260th generation
Chi Chi	60th generation
Loma Prieta	70th generation
Imperial Valley	50th generation
Hollister	50th generation
Kocaeli	55th generation
Trinidad	50th generation
Landers	180th generation
Friuli	70th generation

To conclude this numerical study, Table 12 summarizes the comparison of optimization methods used for positioning control systems. Each method offers distinct advantages, and its suitability depends on factors such as the structure's complexity, the performance goals of the control system, and the available resources for analysis and simulation

Table 12. Optimal position for 3AT, 3TMD and 3ATMD under different earthquakes

Criteria	Modal Controllability	Controllability Index	Genetic Algorithm
Advantages	- Easy to calculate and understand. - Good for preliminary analysis.	- Provides a quantitative measure of control effectiveness. - Can be applied to complex systems.	- Highly flexible, capable of finding optimal solutions in complex search spaces. - Can simultaneously optimize multiple parameters (placement, number of actuators).
Disadvantages	- May not suffice for complex structures or specific performance criteria. - Ignores non-linarites.	- More complex calculations than modal controllability. - May require adjustments for specific structures.	- Requires a significant number of iterations to converge to a solution. - Can be sensitive to algorithm parameters (mutation rate, population size).
Applications	- Initial analysis of control device distribution. - Feasibility studies. - Limited DOFs.	- Detailed control system design for specific structures. - Evaluating the efficiency of different control configurations. - Regular structure.	- Global optimization of control device placement and number in complex structures. - Finding innovative solutions not apparent through classical methods.

6. Conclusions

It is now possible to transform civil engineering structures into smart structures by integrating various control systems, as highlighted in the title of this paper. This study employed methods such as modal controllability, controllability index, and genetic algorithms to identify the optimal placement for active tendons and other control systems within frame structures. Of the three methods explored, the genetic algorithm was retained for its advantage in conducting an extensive parametric study. The MATLAB toolbox was used to implement a multi-objective genetic algorithm to find the best solutions. The findings of the research are summarized into two primary segments:

Part one:

- AT offers a more cost-effective and simpler alternative to TMD and ATMD, with optimal performance achieved when placed in the lower half of the building.
- The placement of ATs significantly influences their effectiveness in structural control. Identifying the optimal position within the building is crucial for maximizing control efficiency.
- Specific locations within the structure are more advantageous for reducing structural response, with optimal placement leading to significant displacement reductions.
- Strategically placed ATs can achieve displacement reductions comparable to those obtained with TMD.
- The ideal placement is determined by two key factors: minimizing the structure's maximum displacement and optimizing the efficiency of the control force generated by ATs;

Part two:

- Installing ATs on half of the building's floors significantly reduces the displacement at the top floor for considered scenarios. However, extending AT installation to all floors results in only a marginal additional reduction of 3% to 5% in displacement. This suggests that further deployment of ATs beyond half of the floors is not economically justifiable.
- The variation in seismic signals demonstrates that the optimal placement of control systems remains largely unaffected by the type of seismic excitation. However, it confirms that certain floors within the structure provide better control effectiveness.
- A careful and systematic analysis of optimal placement, using contemporary methodologies like GA, is crucial to avoid arbitrary positioning of control systems. The research suggests that the lower half of the building is the most effective location for placing ATs in regular structures. For passive control systems like TMD or hybrid systems like ATMD, the top floors (especially the top two floors) offer enhanced performance.
- Additional control devices should be strategically placed where they maximize the damping rate of the fundamental mode, as this mode typically dominates the structural deflection of multi-storey buildings.
- The findings consistently indicate that ATs are most effectively placed on the lower floors of the building

7. Declarations

7.1. Author Contributions

Conceptualization, H.C. and A.M.; methodology, H.C.; software, H.C.; validation, H.C.; formal analysis, H.C. and A.M.; investigation, H.C., A.M., and Z.B.; resources, H.C., A.M., and Z.B.; data curation, H.C.; writing—original draft preparation, H.C.; writing—review and editing, A.M. and Z.B.; visualization, H.C.; supervision, A.M. and Z.B.; project administration, A.M. All authors have read and agreed to the published version of the manuscript.

7.2. Data Availability Statement

The data presented in this study are available in the article.

7.3. Funding

The authors received no financial support for the research, authorship, and/or publication of this article.

7.4. Acknowledgements

The authors would like to express their sincere appreciation to the RISAM laboratory at the University of Tlemcen and the Directorate-General for Scientific Research and Technological Development (DG-SRTD-Algeria) for their invaluable support of this research.

7.5. Conflicts of Interest

The authors declare no conflict of interest.

8. References

[1] Yanik, A., Aldemir, U., & Bakioglu, M. (2011). Energy-based evaluation of seismic response of structures with passive and active systems. WIT Transactions on the Built Environment, 120, 67–78. doi:10.2495/ERES110061.

[2] Berglund, E. Z., Monroe, J. G., Ahmed, I., Noghabaei, M., Do, J., Pesantez, J. E., Khaksar Fasaee, M. A., Bardaka, E., Han, K., Proestos, G. T., & Levis, J. (2020). Smart Infrastructure: A Vision for the Role of the Civil Engineering Profession in Smart Cities. Journal of Infrastructure Systems, 26(2), 03120001. doi:10.1061/(asce)is.1943-555x.0000549.

[3] Ramírez-Neria, M., Morales-Valdez, J., & Yu, W. (2022). Active vibration control of building structure using active disturbance rejection control. JVC/Journal of Vibration and Control, 28(17–18), 2171–2186. doi:10.1177/10775463211009377.

[4] Askari, M., Li, J., & Samali, B. (2017). Cost-effective multi-objective optimal positioning of magnetorheological dampers and active actuators in large nonlinear structures. Journal of Intelligent Material Systems and Structures, 28(2), 230–253. doi:10.1177/1045389X16649449.

[5] Jasiński, M., Salamak, M., & Gerges, M. (2024). Tendon layout optimization in statically indeterminate structures using neural networks and genetic algorithm. Engineering Structures, 305. doi:10.1016/j.engstruct.2024.117713.

[6] Block, P., Boller, G., DeWolf, C., Pauli, J., & Kaufmann, W. (2024). Modelling of prestress losses in 3D tendon layout optimization using strain energy minimization. Proceedings of the IASS 2024 Symposium, 26-30 August, 2024, Zurich, Switzerland.

[7] Jiwapatria, S., Setio, H. D., Sidi, I. D., & Kusumaningrum, P. (2024). Multi-objective optimization of active control system using population guidance and modified reference-point-based NSGA-II. Results in Control and Optimization, 16(June), 100453. doi:10.1016/j.rico.2024.100453.

[8] Zhao, W., & Gu, L. (2023). Hybrid Particle Swarm Optimization Genetic LQR Controller for Active Suspension. Applied Sciences (Switzerland), 13(14), 8204. doi:10.3390/app13148204.

[9] Li, Q. S., Liu, D. K., Tang, J., Zhang, N., & Tam, C. M. (2004). Combinatorial optimal design of number and positions of actuators in actively controlled structures using genetic algorithms. Journal of Sound and Vibration, 270(4–5), 611–624. doi:10.1016/S0022-460X(03)00130-5.

[10] Rama Mohan Rao, A., & Sivasubramanian, K. (2008). Optimal placement of actuators for active vibration control of seismic excited tall buildings using a multiple start guided neighbourhood search (MSGNS) algorithm. Journal of Sound and Vibration, 311(1–2), 133–159. doi:10.1016/j.jsv.2007.08.031.

[11] Pourzeynali, S., Lavasani, H. H., & Modarayi, A. H. (2007). Active control of high rise building structures using fuzzy logic and genetic algorithms. Engineering Structures, 29(3), 346–357. doi:10.1016/j.engstruct.2006.04.015.

[12] Salvi, J., Pioldi, F., & Rizzi, E. (2018). Optimum Tuned Mass Dampers under seismic Soil-Structure Interaction. Soil Dynamics and Earthquake Engineering, 114(July), 576–597. doi:10.1016/j.soildyn.2018.07.014.

[13] Gutierrez Soto, M., & Adeli, H. (2013). Placement of control devices for passive, semi-active, and active vibration control of structures. Scientia Iranica, 20(6), 1567–1578.

[14] Cha, Y. J., Agrawal, A. K., Kim, Y., & Raich, A. M. (2012). Multi-objective genetic algorithms for cost-effective distributions of actuators and sensors in large structures. Expert Systems with Applications, 39(9), 7822–7833. doi:10.1016/j.eswa.2012.01.070.

[15] Liu, D. K., Yang, Y. L., & Li, Q. S. (2003). Optimum positioning of actuators in tall buildings using genetic algorithm. Computers and Structures, 81(32), 2823–2827. doi:10.1016/j.compstruc.2003.07.002.

[16] Cheng, F. Y., Jiang, H., & Zhang, X. (2002). Optimal placement of dampers and actuators based on stochastic approach. Earthquake Engineering and Engineering Vibration, 1(2), 237–249. doi:10.1007/s11803-002-0069-y.

[17] Wani, Z. R., & Tantray, M. (2022). Study on integrated response-based adaptive strategies for control and placement optimization of multiple magneto-rheological dampers-controlled structure under seismic excitations. JVC/Journal of Vibration and Control, 28(13–14), 1712–1726. doi:10.1177/10775463211000483.

[18] Yanik, A., Aldemir, U., & Bakioglu, M. (2014). A new active control performance index for vibration control of three-dimensional structures. Engineering Structures, 62–63, 53–64. doi:10.1016/j.engstruct.2014.01.009.

[19] Zhang, J., Zhu, Y., Li, Z., & Tu, J. (2022). Research on optimal placement of actuators of high-rise buildings considering the influence of seismic excitation on structural modes. Buildings, 12(1), 8. doi:10.3390/buildings12010008.

[20] Rather, F., & Alam, M. (2021). Active seismic control strategy for comparable simultaneous reductions of more than one response. Asian Journal of Civil Engineering, 22(5), 929–940. doi:10.1007/s42107-021-00355-2.

[21] Zhou, C., Liu, Y., Wu, J., & Zhou, C. (2020). Optimal Sensor Placement and Minimum Number Selection of Sensors for Health Monitoring of Transmission Towers. Shock and Vibration, 2375947. doi:10.1155/2020/2375947.

[22] Mei, Z., Guo, Z., Chen, L., Wang, H., & Gao, Y. (2020). Genetic algorithm-based integrated optimization of active control systems for civil structures subjected to random seismic excitations. Engineering Optimization, 52(10), 1700–1719. doi:10.1080/0305215X.2019.1677632.

[23] Hamdaoui, K., Benadla, Z., Chitaoui, H., & Benallal, M. E. (2019). Dynamic behavior of a seven century historical monument reinforced by shape memory alloy wires. Smart Structures and Systems, 23(4), 337–345. doi:10.12989/sss.2019.23.4.337.

[24] Pioldi, F., Salvi, J., & Rizzi, E. (2017). Refined FDD modal dynamic identification from earthquake responses with Soil-Structure Interaction. International Journal of Mechanical Sciences, 127, 47–61. doi:10.1016/j.ijmecsci.2016.10.032.

[25] Özuygur, A. R., & Gündüz, A. N. (2018). Optimal Control of Structures under Earthquakes Including Soil-Structure Interaction. Journal of Earthquake Engineering, 22(8), 1317–1335. doi:10.1080/13632469.2016.1277567.

[26] Chowdhury, I., Tarafdar, R., Ghosh, A., & Dasgupta, S. P. (2017). Dynamic soil structure interaction of bridge piers supported on well foundation. Soil Dynamics and Earthquake Engineering, 97, 251–265. doi:10.1016/j.soildyn.2017.03.005.

[27] Wang, J., & Chopra, A. K. (2009). Linear analysis of concrete arch dams including dam–water–foundation rock interaction considering spatially varying ground motions. Earthquake Engineering & Structural Dynamics, 39(7), 731–750. doi:10.1002/eqe.968.

[28] Cheng, F. Y., Jiang, H., & Lou, K. (2008). Smart structures: innovative systems for seismic response control. CRC Press, Boca Raton, United States. doi:10.1201/9781420008173.

[29] Etedali, S., Akbari, M., & Seifi, M. (2019). MOCS-based optimum design of TMD and FTMD for tall buildings under near-field earthquakes including SSI effects. Soil Dynamics and Earthquake Engineering, 119, 36–50. doi:10.1016/j.soildyn.2018.12.027.

[30] Liu, M. Y., Chiang, W. L., Hwang, J. H., & Chu, C. R. (2008). Wind-induced vibration of high-rise building with tuned mass damper including soil-structure interaction. Journal of Wind Engineering and Industrial Aerodynamics, 96(6–7), 1092–1102. doi:10.1016/j.jweia.2007.06.034.